ChemComm

COMMUNICATION

View Article Online
View Journal | View Issue

Cite this: *Chem. Commun.*, 2025, **61**, 1427

Received 6th October 2024,
Accepted 13th December 2024

DOI: 10.1039/d4cc05247a

rsc.li/chemcomm

Selectivity promotion of Cu by manganese oxide in hydrogenative ring opening of furfural to pentanediols†

Huixiang Li,‡ Huayang Li,‡ Jun Shen, Changhui Liang, Xiaoqiang Zhang, Wei Zhang, Yongxin Li and Z. Conrad Zhang *

This work reports a targeted activation of C–O–C of furfural alcohol (FA) to produce pentanediols (PeDs) over MnO_2-modified Cu. Infrared spectroscopy revealed the strong interaction of the furan ring and C–O–C of FA with the catalyst surface in a preferred flat adsorption configuration, thus facilitating the activation and cleavage of C–O–C to form PeDs.

Lignocellulosic biomass represents the most abundant and a renewable hydrocarbon source in nature. High value utilization of biomass to produce biofuel and chemicals offers promising potential for future sustainable energy development.[1,2] Biomass refinery often proceeds *via* the transformation of cellulose and hemicellulose to platform chemicals.[3–5] Furfural stands out as one of the most important platform chemicals in biorefinery and is produced by dehydration of pentoses in hemicellulose.[6] In the presence of active groups, C=O, C–O–C, and C=C in furfural, multiple valuable chemicals can be obtained through the hydrogenation of these functional groups.[7] Specifically, the hydrogenation of the C=O group in furfural first produces furfural alcohol (FA), which contains two oxygenated functional groups, *i.e.* C–OH and C–O–C. There are two direct hydrogenation pathways in FA conversion.[8,9] One is the hydrogenolysis of the C–OH of FA to methyl furan (MF). Another pathway involves the ring-opening of FA followed by hydrogenation to pentanediols (PeDs). Selective control of the reaction pathway of FA to a target product, either MF or PeDs, is a critical challenge in catalysis.

PeDs (1,2- and 1,5-pentanediol) are highly valuable products for applications in producing microbicides, cosmetics, polyesters, and plastics. Numerous investigations have been performed for the hydrogenation of furfural to PeDs over supported metal catalysts including Cu, Ru, Pt, and Pd.[10–14] Precious metals interfacing with MoO_x and ReO_x favor the formation of PeDs *via* tetrahydrofurfuryl alcohol (THFA) hydrogenolysis;[15,16] $CuCr_2O_4$ as a non-precious Cu-based catalyst was originally reported to produce PeDs through direct ring-opening of furfuryl alcohol;[17] base additives or supports such as $Al(OH)_3$ or hydrotalcite promote the hydrogenolysis ring-opening of FA to form PeDs.[18,19] Early published works indicated that catalytic species on the surface and the chemical properties of the catalyst surface determine the product selectivity of FA hydrogenation through influencing the adsorption configuration of FA on surfaces.[10,18,20]

The oxygen affinity property of the metal catalyst directly affects the interaction of the oxygenate groups of furanic compounds with the catalyst surface, thus influencing the conversion of the furanic compounds.[21–23] Designing metal oxide additives with appropriate oxygen affinity to modify the surface of non-precious Cu probably modulates the adsorption and activation of the furan ring and C–O–C bond in FA to produce PeDs.[24] The oxygen affinity of the metal oxide can be scaled by the dissociation energy of the metal–oxygen bond.[25,26] In analogy to the efficient $CuCr_2O_4$ catalyst, we select manganese oxide, which has similar oxophilic properties to that of chromium oxide ($\Delta H^{f}_{298K\,Mn-O}$ = 402 kJ mol^{-1}, $\Delta H^{f}_{298K\,Cr-O}$ = 427 kJ mol^{-1}),[25] as an additive to modify the Cu catalyst for furfural selective hydrogenation. We deliberately designed reversed catalysts by modifying Cu with dispersed manganese oxide to study the role of manganese oxide on the selectivity of furfural hydrogenation. The designed reverse catalysts allow for elimination of the effect of different metal sites associated with typical supported metal catalysts, and thus being beneficial to study the role of metal oxide sites. As expected, introducing manganese oxide species on Cu powder greatly improves the ring opening selectivity to PeDs *via* furfuryl alcohol. The interaction of FA with the catalyst surface was also explored to understand the promotion effect of manganese oxide in the hydrogenative ring opening of FA.

The catalytic performance of Cu based catalysts was evaluated in the hydrogenation of FA and furfural. Several solvents were first screened for FA hydrogenation. It is demonstrated

National-Local Joint Engineering Research Center of Biomass Refining and High-Quality Utilization, Institute of Urban and Rural Mining, Changzhou University, Changzhou 213164, China. E-mail: zczhang@yahoo.com

† Electronic supplementary information (ESI) available. See DOI: https://doi.org/10.1039/d4cc05247a

‡ These authors contributed equally to this work.

Table 1 Hydrogenation of furanic compounds over Cu-based catalysts

Entry	Catal.	Feed	Conv. %	Sel. % FA	MF	1,2-PeD	1,5-PeD	Others	Mole ratio (PeDs : MF)
1	Cu powder	FA	6.8	—	75.4	24.6	0	0	0.33
2	MnO_2/Cu powder*	FA	25.7	—	13.5	70.4	4.9	11.1	5.60
3	MnO_2/Cu[a]	FA	81.1	—	14.3	48.9	13.1	23.7	4.30
4	MnO_2/Cu[a]	Furfural	100	42.2	5.1	35.1	8.4	9.2	8.50
5	Cu/SiO_2 + MnO_2	Furfural	100	38.8	18.7	28.4	3.7	11.1	1.70
6	MnO_x/Cu[a]	THFA	0	—	—	0	0	0	

Reaction conditions: catalyst 85 mg, Cu/SiO_2 100 mg; reactant 0.5 g, isopropanol 2 mL, 4.5 MPa H_2, 170 °C, 6 h, *3 h. Others are THFA, 1-pentanol and methyl-tetrahydrofuran. [a] Prepared by leaching Al from MnO_2/CuAl, the MnO_2 loading is 1.3 wt%. 1,2-PeD and 1,5-PeD are the abbreviations of 1,2-pentanediol and 1,5-pentanediol, respectively.

that isopropanol (IPA) exhibits the best performance for this reaction. In other solvents, either the carbon balance of the reaction was low (especially in H_2O, ethyl acetate) or the catalyst activity was low (for instance, in tetrahydrofuran, *N*,*N*-dimethylformamide, CH_3CN) (Fig. S1, ESI†). Table 1 presents the hydrogenation performance for furfural and F in IPA over Cu-based catalysts. Cu powder is efficient for the selective hydrogenolysis of C–OH in FA to form methyl furan (MF) with 75.4% selectivity. 1,2-PeD is produced with a low selectivity of 24.6%. Upon loading MnO_2 on Cu powder through a simple impregnation method, the reaction path of FA hydrogenation shifts to ring-opening to PeDs as the main product with 75.3% selectivity, therein 1,2-PeD is the dominant product. The selectivity ratio of PeDs to MF increased from 0.33 to 5.6. However, the conversion of FA is still limited to less than 30%, probably due to the low surface area of Cu powder (2.2 $m^2\ g^{-1}$). RANEY® Cu with a larger surface area is therefore used to obtain high FA conversion.[27] A manganese precursor (manganous nitrate) was first loaded on a CuAl alloy through impregnation followed by high temperature calcination. Subsequently, the Al was leached with a base (see Experimental section). The amount of MnO_2 on Cu was determined with ion chromatography. The catalytic reactions revealed that moderate loading of MnO_2 (about 1.0 wt%) on Cu is beneficial for selectively producing PeDs (Fig. S2, ESI†). Specifically, 1.3 wt% MnO_2/Cu catalyst exhibited a remarkably high activity in FA hydrogenation (conv. 81.1%), producing PeDs with a selectivity of 62.0% (Table 1, entry 3). A selectivity of PeDs up to 43.5% was also obtained when furfural is used as a reactant. In addition, Table 1 shows that 1,2-PeD represents the dominant ring-opening product from FA hydrogenolysis over Cu derived catalysts. It also exhibits the catalytic performance of a physical mixture of MnO_2 and Cu (entry 5). Slightly increased selectivity of PeDs (32.1%) was achieved, indicating the synergistic catalysis of MnO_2 interfacing Cu species on the surface. Overall, the ring-opening hydrogenation of furfural and FA was promoted by MnO_2 on Cu. Ultimately, the reaction conditions, H_2 pressure and reaction temperature, were optimized. The results indicate that both high H_2 pressure and high temperature are conducive to the hydrogenative ring-opening of furfural to PeDs. The influence of temperature and pressure on the selectivity of MF is relatively insignificant. The selectivity of pentanediols from furfural over MnO_2/Cu reaches up to 58% under 190 °C, 6 MPa H_2 (Fig. S3, ESI†). However, the MnO_2/Cu catalyst fails to catalyze the ring opening of other similar biomass derivatives, such as MF, furan, methyltetrahydrofuran, tetrahydrofurfuryl alcohol, and 5-hydroxymethylfurfural. This is probably due to the fact that various substituents on the furan ring affect its activity and conversion.

To determine the reaction pathway of furfural hydrogenation over the MnO_2/Cu catalyst, we first analyzed the distribution of products at different reaction times. At the initiation of the reaction, furfural was rapidly hydrogenated to FA. As the reaction progressed, FA was gradually consumed, and the quantities of products, *i.e.* MF, THFA and PeDs gradually increased (Fig. S3c, ESI†). This implies that furfural hydrogenation undergoes FA to yield the products (Scheme S1, ESI†). FA hydrogenation to PeDs generally proceeds by two pathways: (1) total hydrogenation of furfural to THFA followed by selective hydrogenolysis of THFA to PeDs; (2) C═O hydrogenation to FA and followed by direct ring-opening to PeDs.[28,29] Entry 6 shows that THFA remained unconverted, suggesting that PeDs were formed *via* the second pathway over the MnO_2/Cu catalyst. In addition, the catalytic performance of MnO_2/Cu in ring opening hydrogenation of furanic compounds was also compared with other reported non-noble metal catalysts in the literature. Apparently, the MnO_2/Cu catalyst displays excellent performance for producing as high as 54% selectivity of PeDs from furfural (Table S1, ESI†). In addition, after reaction for 15 h, only 0.02% of Mn and 0.036% of Cu were detected in the solution, indicating little leaching of the metals. The reusability test showed that the catalytic performance of the MnO_2/Cu catalyst remains stable in five successive runs (Fig. S4, ESI†).

To understand the mechanism on the selective hydrogenative ring opening of FA over MnO_2/Cu, the chemical–physical properties of the catalyst and the catalyst structure, active species and the interaction of FA with the catalyst surface are studied. The local crystalline structures of Cu and MnO_2/Cu were first characterized with XRD, as shown in Fig. 1 and Fig. S5 (ESI†). For Cu powder, the diffraction peaks were observed at 2θ = 43.3, 50.5, 74.1 and 36.4, indicative of the coexistence of Cu and Cu_2O (PDF Cu_2O 96-900-7498). Upon modifying Cu with MnO_2 at different loadings, the peaks of Cu and Cu_2O remained unchanged across all the as-prepared catalysts (Fig. 1). A small peak of MnO_2 at 2θ = 36.4° (PDF 96-900-9112) emerged when the MnO_2 loading was gradually increased to 3.5 wt%, indicating the good dispersion of MnO_2 species on Cu. In addition, the diffraction peak of Al_2O_3 at

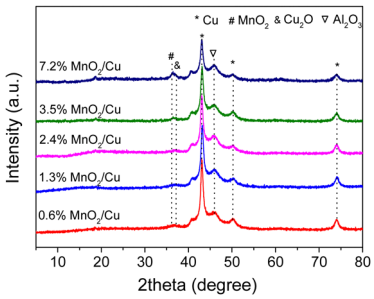

Fig. 1 XRD patterns of MnO_2/Cu with different MnO_2 loading.

2θ = 45.9° was also observed, showing the presence of residual aluminum species after the leaching treatment. However, the catalytic evaluation revealed that Al_2O_3 had no significant role in enhancing the selectivity of PeDs (Table S2, ESI†). Thus, it is likely that three active species, Cu, Cu_2O, and MnO_2, coexist on the catalyst surface. The oxidation state of Mn on the catalyst surface was further verified to be Mn^{4+} through X-ray photoelectron spectroscopy[30,31] (Fig. S6, ESI†). Subsequently, the distribution of the surface species, as well as the structure and morphology was characterized with high resolution scanning and transmission electron microscopy (HRTEM and SEM) images and energy-dispersive X-ray spectroscopy (EDX), as shown in Fig. 2 and Fig. S7 and S8 (ESI†). The size of the catalyst particles is estimated to be in the range of 60–100 nm. The lattices of Cu (111) and Cu_2O (111) are clearly observed on the surface of MnO_2/Cu (Fig. 2c). The percentage of Cu^+ (Cu^+/Cu_{total}) was determined to be 22.5% based on the peak fitting of the Cu LMM spectrum (see Experimental section, Fig. S6, ESI†). In the elemental maps of MnO_2/Cu, the yellow and red dots correspond to the distribution of Cu and Al elements, respectively, suggesting that the Mn species are homogeneously distributed on the Cu (Fig. 2d). Additional images in Fig. S7 and S8 (ESI†) from the examination of different regions also indicate the homogeneous distribution of Mn species and the coexistence of Cu and Cu_2O species on the surface layer. The Cu and Cu_2O species provide the active sites for furfural hydrogenation to FA followed by the hydrogenolysis of the C–OH group of FA to MF. Metallic Cu sites are responsible for the activation of H_2. The adsorption and activation of the C–OH group in FA proceeded on the Cu_2O sites to produce MF.[10,32] It is further demonstrated that MnO_2 species have a promotional impact on the selective hydrogenative ring-opening of FA to 1,2-PeD.

One hypothesis is that the MnO_2 species may induce a change in the oxygen affinity of the catalyst surface, and thus in the interaction of oxygenated functional groups of FA with the surface. The interaction of FA with catalytic sites on the surface determines the reaction selectivity.[23,33] Diffuse reflectance infrared spectroscopy (DRIFT) was carried out to obtain molecular insights into the interaction of FA with the catalyst surface to reveal the promotional effect of MnO_2 sites on the selectivity of PeDs. Fig. 3 shows the infrared spectra of FA adsorbed on Cu and MnO_2/Cu. On the surface of Cu, the absorption bands assigned to the furan ring at 755, 842, 918 and 1021 cm^{-1}, C^5–O at 1077 cm^{-1}, C^1–O–C^4 at 1151 cm^{-1}, and C^2–C^3 at 1221 cm^{-1},[34–36] in FA are observed. Over the surface of MnO_2/Cu, the peaks of furan and C^1–O–C^4 have been red-shifted by approximately 3–18 cm^{-1}, but the position of the C^5–O peak remains unchanged. Thus, the interaction of furan and C^1–O–C^4 with the catalyst was enhanced upon introducing MnO_2 on Cu. Meanwhile, FA adsorption on MnO_2/Cu prefers a flat configuration of the furan ring.[18,35] This adsorption configuration ensures the activation of C^1–O–C^4 and highly selective hydrogenative ring-opening of FA over MnO_2/Cu. The adsorption configuration of FA on the catalyst is probably affected by the oxygen affinity of the metal catalysts.[24,37,38] In the absence of manganese oxide, copper oxide species on the Cu catalyst have weaker oxygen affinity ($\Delta H^f_{298K\,Cu-O}$ = 343 kJ mol^{-1}), resulting in the weaker interaction of C_1–O–C_4 in furan with the Cu catalyst. The oxygen affinity of manganese oxide has a similar value to that of the efficient promoter chromium oxide ($\Delta H^f_{298K\,Mn-O}$ = 402 kJ mol^{-1}, $\Delta H^f_{298K\,Cr-O}$ = 427 kJ mol^{-1}). Other metal oxides, MoO_3, SnO_2, and WO_3 with stronger oxygen affinity ($\Delta H^f_{298K\,Mn-O}$ = 607 kJ mol^{-1}, $\Delta H^f_{298K\,W-O}$ = 653 kJ mol^{-1}, $\Delta H^f_{298K\,Sn-O}$ = 548 kJ mol^{-1})[25] were also studied as additives to explore the influence of the oxygen affinity property in furfural selective hydrogenation. The catalytic results show that MF is the dominant product with quite low selectivity ratio of PeDs to MF (Table S2, ESI†), indicating that the stronger oxygen affinity of metal oxide is favorable for the activation of C–OH to MF but not beneficial for ring-opening of FA.

Overall, Cu nanoparticles contribute to the hydrogenation of furfural and further hydrogenolysis to MF. Upon introducing metal oxide additives on Cu, the conversion path of FA varies from C–OH hydrogenolysis to hydrogenative ring opening. The oxygen affinity of metal oxides greatly influences the reaction pathway and product selectivity, through affecting the interaction

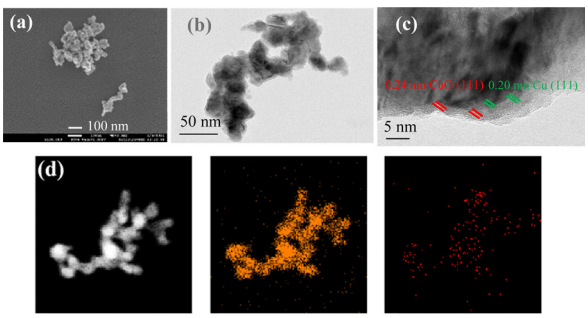

Fig. 2 HAADF-STEM images (a)–(c) and EDX mapping images (d) of the MnO_2/Cu catalyst.

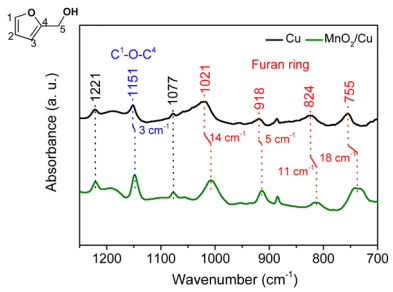

Fig. 3 Infrared spectra of FA adsorbed on Cu and MnO_2/Cu.

of oxygenate groups in FA with the catalyst surface. Metal oxides, *e.g.* MoO_3, SnO_2, and WO_3 with stronger oxygen affinity properties are favorable for the activation of C–OH to MF; metal oxide, *e.g.* MnO_2 with moderate strong oxygen affinity benefits the ring-opening of FA to PeDs. Characterization results reveal that MnO_2 sites on Cu promote the interaction of the furan ring and C–O–C with the catalyst by a flat adsorption configuration, thus favoring the activation and cleavage of C–O–C, forming the hydrogenative ring-opening product.

In summary, this work shows the selective hydrogenation of furan compounds, furfural and FA, over non-noble metal catalysts. The Cu catalyst facilitates the production of MF. The introduction of MnO_2 on Cu significantly enhanced the selectivity of ring-opening to PeDs, resulting in at least thirteen times increase of the PeDs/MF ratio. Characterization results reveal the homogeneous distribution of Mn species and the coexistence of Cu and Cu_2O species on the catalyst surface. The adsorption of furan compounds on the catalyst surface directly determines the activation of functional groups of reactants. The furan ring and C–O–C of FA prefer to interact with the catalyst surface in a flat adsorption configuration upon modifying Cu with MnO_2, and this contributes to the activation of C–O–C and the formation of ring-opening products, PeDs. This work offers new metrics on the importance of applying the oxygen affinity property to design efficient and non-precious catalysts for the selective hydrogenolysis of biomass-derived furan compounds to pentanediols.

Huixiang Li and Z. Conrad Zhang designed the research. Huixiang Li conducted the catalyst preparation and reaction evaluation, analyzed the data, and wrote the paper. Huayang Li and Jun Shen did the reaction evaluation. Changhui Liang, Xiaoqiang Zhang and Yongxin Li discussed the results, and commented on the paper. All authors have given approval to the final version of the manuscript.

This work was supported by the National Natural Science Foundation of China (22202196, 21932005, 22172164), Changzhou Sci&Tech Program (Grant No. CQ20230091, CJ20241088), and Jiangsu Provincial Department of Science and Technology (BX2023015).

Data availability

The data supporting this article have been included as part of the ESI.†

Conflicts of interest

There are no conflicts to declare.

Notes and references

1 Z. Guzovic, N. Duic, A. Piacentino, N. Markovska, B. V. Mathiesen and H. Lund, *Energy*, 2022, **245**, 123276.
2 J. Ma, S. Shi, X. Jia, F. Xia, H. Ma, J. Gao and J. Xu, *J. Energy Chem.*, 2019, **36**, 74–86.
3 Z. Zhou, D. Liu and X. Zhao, *Renewable Sustainable Energy Rev.*, 2021, **146**, 111169.
4 Y. Liu, Y. Nie, X. Lu, X. Zhang, H. He, F. Pan, L. Zhou, X. Liu, X. Ji and S. Zhang, *Green Chem.*, 2019, **21**, 3499–3535.
5 P. Gallezot, *Chem. Soc. Rev.*, 2012, **41**, 1538–1558.
6 C. Xu, E. Paone, D. Rodriguez-Padron, R. Luque and F. Mauriello, *Chem. Soc. Rev.*, 2020, **49**, 4273–4306.
7 Y. Wang, D. Zhao, D. Rodríguez-Padrón and C. Len, *Catalysts*, 2019, **9**, 796–828.
8 K. Yan, G. Wu, T. Lafleur and C. Jarvis, *Renewable Sustainable Energy Rev.*, 2014, **38**, 663–676.
9 H. Liu, Z. Huang, H. Kang, C. Xia and J. Chen, *Chin. J. Catal.*, 2016, **37**, 700–710.
10 S. Chen, R. Wojcieszak, F. Dumeignil, E. Marceau and Sb Royer, *Chem. Rev.*, 2018, **118**, 11023.
11 R. Ma, X. Wu, T. Tong, Z. Shao, Y. Wang, X. Liu, Q. Xia and X. Gong, *ACS Catal.*, 2017, **7**, 333–337.
12 B. Zhang, Y. Zhu, G. Ding, H. Zheng and Y. Li, *Green Chem.*, 2012, **14**, 3402–3409.
13 F. Gao, H. Liu, X. Hu, J. Chen, Z. Huang and C. Xia, *Chin. J. Catal.*, 2018, **39**, 1711–1723.
14 J. Lee, J. Woo, C. Nguyen-Huy, M. S. Lee, S. H. Joo and K. An, *Catal. Today*, 2020, **350**, 71–79.
15 Y. Nakagawa, M. Tamura and K. Tomishige, *Catal. Surv. Asia*, 2015, **19**, 249–256.
16 S. Koso, Y. Nakagawa and K. Tomishige, *J. Catal.*, 2011, **280**, 221–229.
17 H. A. A. R. Connor, *J. Am. Chem. Soc.*, 1931, **53**, 1091–1095.
18 H. Li, X. Nie, H. Du, Y. Zhao, J. Mu and Z. C. Zhang, *ChemSusChem*, 2023, DOI: **10.1002/cssc.202300880**.
19 T. Mizugaki, T. Yamakawa, Y. Nagatsu, Z. Maeno, T. Mitsudome, K. Jitsukawa and K. Kaneda, *ACS Sustainable Chem. Eng.*, 2014, **2**, 2243–2247.
20 R. Šivec, M. Huš, B. Likozar and M. Grilc, *Chem. Eng. J.*, 2022, **436**, 135070.
21 P. M. de Souza, R. C. Rabelo-Neto, L. E. P. Borges, G. Jacobs, B. H. Davis, D. E. Resasco and F. B. Noronha, *ACS Catal.*, 2017, **7**, 2058–2073.
22 Q. Tan, G. Wang, A. Long, A. Dinse, C. Buda, J. Shabaker and D. E. Resasco, *J. Catal.*, 2017, **347**, 102–115.
23 C. A. Teles, P. M. de Souza, A. H. Braga, R. C. Rabelo-Neto, A. Teran, G. Jacobs, D. E. Resasco and F. B. Noronha, *Appl. Catal., B*, 2019, **249**, 292–305.
24 P.-J. Hsu, J.-W. Jiang and Y.-C. Lin, *ACS Sustainable Chem. Eng.*, 2017, **6**, 660–667.
25 J. A. Dean, *Lange's Handbook of Chemistry*, R. R. Donnelley & Sons Company, 15th edn, 1934.
26 K. A. Moltved and K. P. Kepp, *J. Phys. Chem. C*, 2019, **123**, 18432–18444.
27 M. S. Wainwright and R. B. Anderson, *J. Catal.*, 1980, **64**, 124–131.
28 Z. J. Brentzel, K. J. Barnett, K. Huang, C. T. Maravelias, J. A. Dumesic and G. W. Huber, *ChemSusChem*, 2017, **10**, 1351–1355.
29 D. S. Pisal and G. D. Yadav, *ACS Omega*, 2019, **4**, 1201–1214.
30 H. W. Nesbitt and D. Banerjee, *Am. Mineral.*, 1998, **83**, 305–315.
31 P. Dubot, D. Jousset, V. Pinet, F. Pellerin and J. P. Langeron, *Surf. Interface Anal.*, 1988, **12**, 99–104.
32 H. Du, X. Ma, P. Yan, M. Jiang, Z. Zhao and Z. C. Zhang, *Fuel Process. Technol.*, 2019, **193**, 221–231.
33 P. M. de Souza, R. C. Rabelo-Neto, L. E. P. Borges, G. Jacobs, B. H. Davis, T. Sooknoi, D. E. Resasco and F. B. Noronha, *ACS Catal.*, 2015, **5**, 1318–1329.
34 Y. Zhu, W. Zhao, J. Zhang, Z. An, X. Ma, Z. Zhang, Y. Jiang, L. Zheng, X. Shu, H. Song, X. Xiang and J. He, *ACS Catal.*, 2020, **10**, 8032–8041.
35 Z. Tong, X. Li, J. Dong, R. Gao, Q. Deng, J. Wang, Z. Zeng, J.-J. Zou and S. Deng, *ACS Catal.*, 2021, **11**, 6406–6415.
36 Y. Shao, J. Wang, H. Du, K. Sun, Z. Zhang, L. Zhang, Q. Li, S. Zhang, Q. Liu and X. Hu, *ACS Sustainable Chem. Eng.*, 2020, **8**, 5217–5228.
37 H. Li, P. Yan, B.-Q. Xu and Z. Conrad Zhang, *J. Catal.*, 2022, **412**, 21–29.
38 Y. Li, B. Liu, Y. Wang, S. Wang, X. Lan and T. Wang, *ACS Catal.*, 2022, **12**, 7926–7935.

